nature physics

SUPPLEMENTARY INFORMATION

DOI: 10.1038/NPHYS4142

In the format provided by the authors and unedited.

Separating the configurational and vibrational entropy contributions in metallic glasses

Hillary L. Smith,[1] Chen W. Li,[2] Andrew Hoff,[1] Glenn R. Garrett,[1] Dennis S. Kim,[1] Fred C. Yang,[1] Matthew S. Lucas,[3] Tabitha Swan-Wood,[4] J.Y.Y. Lin,[5] M.B. Stone,[6] D.L. Abernathy,[6] Marios D. Demetriou,[1] and B. Fultz[1]

[1] *California Institute of Technology, Department of Applied Physics and Materials Science, Pasadena, California 91125, USA*

[2] *University of California Riverside, Department of Mechanical Engineering, Riverside, California 92521, USA*

[3] *Air Force Research Laboratory, Wright-Patterson AFB, Ohio 45433 USA*

[4] *California State University Channel Islands, Department of Applied Physics, Camarillo, California 93012, USA*

[5] *Neutron Data Analysis and Visualization Division, Oak Ridge National Laboratory, Oak Ridge, Tennessee 37831, USA*

[6] *Quantum Condensed Matter Division, Oak Ridge National Laboratory, Oak Ridge, Tennessee 37831, USA*

(Dated: February 17, 2017)

In-situ Neutron Diffraction

Diffraction patterns can be obtained from elastic scattering that is acquired at the same time as the inelastic neutron scattering used for the phonon densities of states. Integration of the intensity around the elastic peak provides diffraction patterns as shown in Fig. 1. During the in-situ neutron experiments, the sample is initially fully amorphous. It is then continuously heated through the glass transition and through crystallization. This evolution is visible from the neutron diffraction as new crystalline peaks appear at the onset of crystallization.

In Fig. 1, intensity is plotted as a function of Q, with additional scans offset to more clearly show changes in the peaks. For each material, the glass is fully amorphous in the bottom (blue) scan and temperature increases in successive scans until the material crystallizes. The top scan (red) shows the crystalline material. For each material, a region of Q is highlighted to the right where new Bragg peaks appear from crystallization.

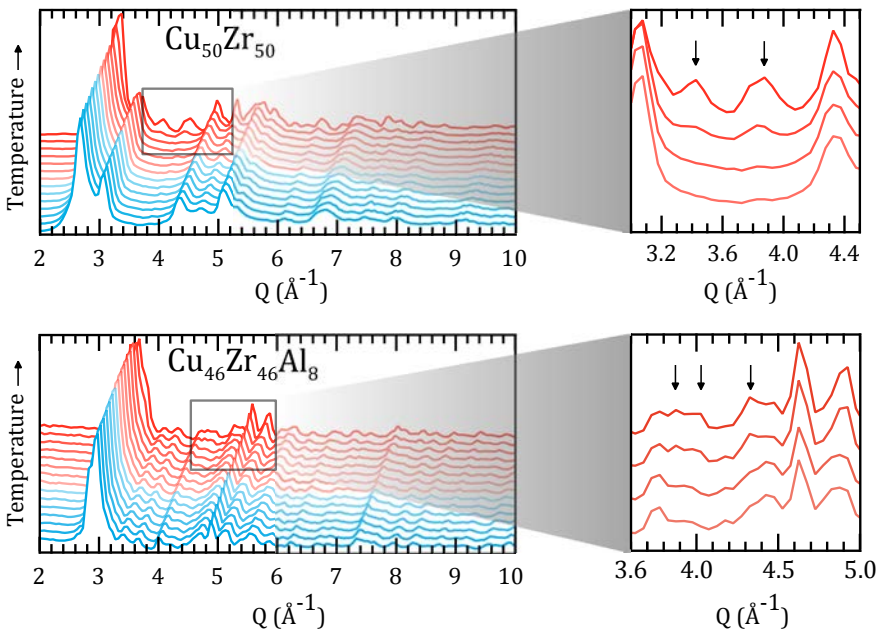

FIG. 1. **In-situ Neutron Diffraction of $Cu_{50}Zr_{50}$ and $Cu_{46}Zr_{46}Al_8$.** Elastic scattering as a function of momentum transfer Q from continuous heating from the amorphous state (blue) through the glass transition and crystallization. The emergence of diffraction peaks from the amorphous phase to complete crystallization is highlighted to the right for each material with crystalline peaks from the sample indicated with arrows.

Background scattering from the sample environment and sample holder was not removed, producing the large number of peaks visible in both datasets. $Cu_{50}Zr_{50}$ was measured in a low-mass electrical resistance furnace with aluminum shielding and aluminum sample holder, contributing aluminum diffractions. $Cu_{46}Zr_{46}Al_8$ were measured in an electrical resistance furnace (MICAS furnace) with vanadium shielding and a niobium sample holder, contributing niobium diffractions (vanadium has a negligible coherent scattering cross section). Despite these background diffractions, the crystallization of the amorphous material is clear from the decrease in the amorphous peak, and evolution of crystalline peaks.

Calorimetry

Differential scanning calorimetry scans for both materials at 20 K per minute are shown in Fig. 2. The features of the glass transition, crystallization, the B2 phase transformation, and melting are indicated with arrows.

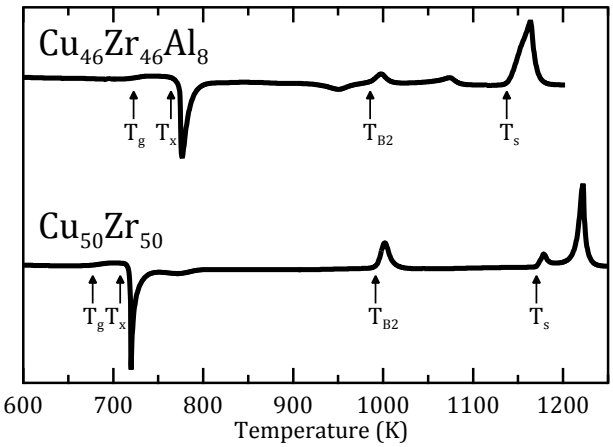

FIG. 2. **Differential scanning calorimetry of amorphous $Cu_{50}Zr_{50}$ and $Cu_{46}Zr_{46}Al_8$ at a heating rate of 20K per min.** The glass transition is characterized by an endothermic rise in heat capacity, followed by the sharp exothermic peak of crystallization. The glass transition and crystallization temperatures, T_g and T_x, are indicated by arrows.

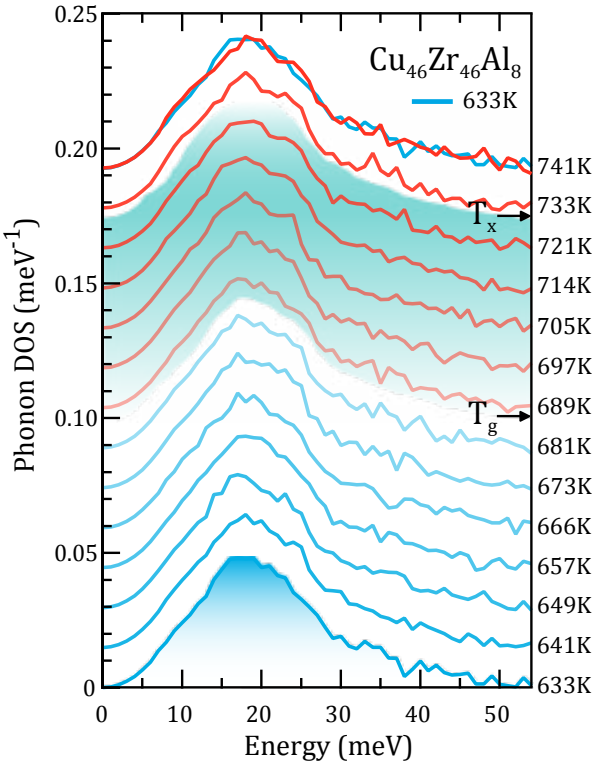

FIG. 3. **Phonon DOS curves of $Cu_{46}Zr_{46}Al_8$.** DOS curves were obtained during the heating of from the amorphous state, through the glass transition, and above crystallization. The shaded region indicates the temperature range where the material is in the undercooled liquid. The 633 K DOS of the amorphous phase (shaded blue) is shown also at high temperature, overlaid with the DOS of the crystalline phase at 741 K.

Phonon Densities of States

Figure 3 shows phonon DOS curves during the heating of $Cu_{46}Zr_{46}Al_8$ from the amorphous state (blue) through the glass transition and above crystallization. Data were acquired during continuous heating at 2 K per min and binned in 8 K intervals. Each spectrum was acquired in 3-5 minutes. The 633 K DOS of the amorphous phase (shaded blue) is shown also at high temperature, overlaid with the DOS of the crystalline phase at 741 K. The shaded region indicates the temperature range where the material is in the undercooled liquid. The DOS curves show little change with temperature during heating through the undercooled liquid. The spectrum at the highest temperature shows a small change after crystallization.